A&A 529, A24 (2011)
DOI: 10.1051/0004-6361/201014423

Astronomy & Astrophysics

Orion KL: the hot core that is not a "hot core"

L. A. Zapata[1,2], J. Schmid-Burgk[1], and K. M. Menten[1]

[1] Max-Planck-Institut für Radioastronomie, Auf dem Hügel 69, 53121 Bonn, Germany
e-mail: lzapata@mpifr-bonn.mpg.de
[2] Centro de Radioastronomía y Astrofísica, Universidad Nacional Autónoma de México, Morelia 58090, México

Received 12 March 2010 / Accepted 11 January 2011

ABSTRACT

We present sensitive high angular resolution submillimeter and millimeter observations of torsionally/vibrationally highly excited lines of the CH_3OH, HC_3N, SO_2, and CH_3CN molecules and of the continuum emission at 870 and 1300 μm from the Orion KL region, made with the Submillimeter Array (SMA). These observations and SMA CO $J = 3-2$ and $J = 2-1$ imaging of the explosive flow originating in this region suggest that the molecular Orion "hot core" is a pre-existing density enhancement heated from the outside by the explosive event. Unlike in other hot cores, we do not find any self-luminous submillimeter, radio, or infrared source embedded in the hot molecular gas, nor observe filamentary CO flow structures or "fingers" in the shadow of the hot core pointing away from the explosion center. The low-excitation CH_3CN emission shows the typical molecular heart-shaped structure, traditionally named the hot core, and is centered close to the dynamical origin of the explosion. The highest excitation CH_3CN lines all originate from the northeast lobe of the heart-shaped structure, i.e. from the densest and most highly obscured parts of the extended ridge. The torsionally excited CH_3OH and vibrationally excited HC_3N lines appear to form a shell around the strongest submillimeter continuum source. All of these observations suggest that the southeast and southwest sectors of the explosive flow have impinged on a pre-existing very dense part of the extended ridge, thus creating the bright Orion KL hot core. However, additional theoretical and observational studies are required to test this new heating scenario.

Key words. molecular data – methods: observational – techniques: interferometric – ISM: jets and outflows – ISM: molecules – ISM: kinematics and dynamics

1. Introduction

The famous eponymous hot core in the Orion Kleinmann-Low (KL) star-forming region was given its name by Ho et al. (1979), who identified it as a compact source of hot ammonia emission embedded in a more extended ridge of dense material. A few years later, Pauls et al. (1983), using the early *Very Large Array (VLA)* at 2″ resolution, showed the hot ammonia to arise from a heart-shaped region of size ≈15″ × 15″ or 0.03 × 0.03 pc^2 at a distance of 414 pc (Menten et al. 2007).

Early millimeter interferometry with the Hat Creek Millimeter Interferometer (later Berkeley-Illinois-Maryland Array, BIMA) and the Owens Valley Radio Observatory (OVRO) Millimeter Array showed a chemically and dynamically complex picture for the Orion hot core and (at least) one other conspicuous region abutting it, the "compact ridge". Many molecular lines arising from lower and moderately excited levels above the ground state also showed the peculiar "heart" or "U" morphology, for example CO, HCN, CH_3CN, $H^{13}CN$, HNCO, OCS, HDO, SO, and SO_2 (Genzel et al. 1982; Migenes et al. 1989; Wilner et al. 1994; Wright et al. 1996; Blake et al. 1996; Chernin & Wright 1996; Wilson et al. 2000; Friedel & Snyder 2008). The LSR velocities had a centroid between 6 and 8 km s^{-1}, close to the velocity of the ambient larger-scale ridge material (~9 km s^{-1}).

The heart-shaped structure occupies an area between two of the bona fide self-luminous sources in the region, source *I* and the Becklin-Neugebauer object (*BN*), which both exhibit weak radio emission.

Most of the molecules, as the NH_3, C_5H_3CN, CH_2H_3CN, $(CH_3)_2CO$, HCOOH, and $HCOOCH_3$, if imaged with higher resolution exhibit a clumpy structure of a different morphology but always well placed inside the area drawn by the heart-shaped structure (Blake et al. 1996; Liu et al. 2002; Friedel & Snyder 2008). These molecular clumps show complex dynamics without any special trend other than their emission velocity centroid being close to the systemic velocity (Masson & Mundy 1988; Wilner et al. 1994; Liu et al. 2002; Friedel & Snyder 2008).

Soon after the first identification of the Orion hot core, hot (~150 K), compact (<0.05 pc), dense (10^6 cm^{-3}) cores with elevated abundances of many molecules were discovered in other regions. These physical parameters are not generalized, in the past few decades, different values have been found. One of the first measurements was that obtained using the Hat Creek interferometer close (0.07 pc) to the archetypical ultracompact HII region W3OH (Turner & Welch 1984; Mauersberger et al. 1986). Subarcsecond resolution millimeter interferometry with the IRAM Plateau de Bure Interferometer resolved the "Turner-Welch object" into a protocluster consisting of three sources (Wyrowski et al. 1999), one of which drives a powerful H_2O maser outflow and two of which are associated with weak radio continuum emission. Many more hot cores with characteristics similar to the above-mentioned were found thereafter, all of which appear to host one or more of the following: a hyper/ultra-compact HII region, a strong millimeter source, a compact H_2O maser outflow, and/or a class II CH_3OH maser (for reviews, see Kurtz et al. 2000; Cesaroni 2005). For an example, we refer to the compact hot cores associated with intermediate mass protostars located just 0.15 pc south of KL in Orion South (Zapata et al. 2007). Hot cores have even been found powered by solar mass protostars, i.e. the so-called "hot corinos" (Ceccarelli et al. 2000; Bottinelli et al. 2004).

Table 1. Observational and physical parameters of submillimeter and millimeter lines.

Lines	Rest frequency [GHz]	$E_{\rm lower}/k$ [K]	Range of velocities [km s^{-1}]	Linewidth[a] [km s^{-1}]	LSR velocity [km s^{-1}]	Peak flux [Jy Beam^{-1}]
$CH_3CN(12_3–11_3)$	220.7090...	122	−10, +26	18	7	17
$CH_3CN(12_6–11_6)$	220.5944...	315	−5, +15	13	5	12
$CH_3CN(12_9–11_9)$	220.4039...	636	+2, +12	4	6	1
$CH_3OH(7_{4,3}–6_{4,3})$ A$^-$ ($\nu_t = 1$)	337.9694...	373	−5, +15	5	8	13
$CH_3OH(7_{4,3}–6_{4,3})$ A$^-$ ($\nu_t = 2$)	337.8775...	705	−2, +11	4	8	3
$HC_3N(37–36)(\nu_7 = 1)$	337.8240...	613	−12, +19	14	4	8
$SO_2(21_{2,20}–21_{1,21})(\nu_2 = 1)$	337.8925...	948	−1, +13	5	6	2

Notes. [(a)] For the $HC_3N(37–36)$ and $CH_3OH(7_{4,3}–6_{4,3})$ A$^-$ ($\nu_t = 1$) torsionally/vibrationally excited lines the average linewidth given here is the sum of two velocity components, one centered at approximately −4 km s^{-1} and the other one at +7 km s^{-1}.

In contrast, what is heating the hot core in the Orion KL region and whether, in particular, this core harbors (a) proto- or young stellar object(s) have been debated for a long time.

Blake et al. (1996), using line and continuum observations with OVRO, found no evidence of a luminous internal heating source within the Orion KL hot core. BIMA observations of formic acid (HCOOH) and the positions of H_2O masers (see e.g. Genzel et al. 1981; Gaume et al. 1998) in the compact ridge region suggested that these molecules delineate the interaction region between the Orion KL outflow and the ambient quiescent gas (Liu et al. 2002). Chernin & Wright (1996) found that their CO data were consistent with a northwest-southeast biconical outflow centered close to the positions of *BN* and source *I* that is partly truncated by the hot core. This is quite suggestive of the outflow's energy being partly dissipated in heating the Orion KL hot core.

On the other hand, Kaufman et al. (1998) proposed that the Orion KL hot core is more likely to be heated by stars embedded within the core rather than that by an external source because of the core's large column densities ($N(H_2) \geq 10^{23}$ cm^2) and warm temperatures ($T \geq 100$ K). In addition, the distribution of vibrationally excited HC_3N emission suggests that the Orion hot core is heated from inside by a group of stars (de Vicente et al. 2002).

A group of strong near- and mid-infrared sources have been proposed to be responsible for heating the Orion KL hot core and the compact ridge (Genzel & Stutzki 1989; Blake et al. 1996). However, sensitive VLA radio observations made by Menten & Reid (1995) revealed that most of the IR sources in the Orion KL nebula are not self-luminous but rather show reprocessed emission escaping through inhomogeneities in the dense material. In particular, these data showed that no part of the "IRc2" group of IR sources was coincident with the conspicuous radio continuum source *I* that lies within the boundaries but not at the center of the heart-shaped molecular structure. Furthermore, OVRO and CARMA millimeter continuum maps compiled by Blake et al. (1996); Friedel & Snyder (2008) demonstrated that the millimeter and IR sources do not show good correspondence. In addition, Blake et al. (1996); Wright et al. (1996); Chandler & Wood (1997) found that the dust and the peak molecular emission coincide with neither source *I* nor IRc2, the radio and infrared sources closest to the hot core.

In this paper, we present sensitive high angular resolution submillimeter and millimeter observations of the Orion KL region that were made in an attempt to understand the nature of the hot molecular material it harbors. We used the Submillimeter Array to image the continuum at 870 and 1300 μm and a series of molecular lines emitted from energy levels with moderate, high, and very high energies (122–948 K) above the ground state, namely CH_3OH in the first and the second torsionally excited states, HC_3N and SO_2 in vibrationally excited states and high excitation lines from the vibrational ground state of CH_3CN.

In Sect. 2, we discuss the observations, in Sect. 3 we present and discuss our SMA millimeter and submillimeter data. Finally, in Sect. 4 we give the main conclusions drawn from the observations.

2. Observations

2.1. Millimeter

Observations were made with the Submillimeter Array[1] (SMA) during 2007 January and 2009 February. The SMA was in its compact and sub-compact configurations with baselines ranging in projected length from 6 to 58 kλ. We used the mosaicking mode with half-power point spacing between field centers and covered the entire Orion hot core. The primary beam of each pointing at 230 GHz has a $FWHM$ diameter of about 50″.

The receivers were tuned to a frequency of 230.5387970 GHz in the upper sideband (USB), while the lower sideband (LSB) was centered on 220.5387970 GHz. The $CH_3CN(12_k–11_k)$ k-ladder with $k = 10, \ldots, 1, 0$ was detected in the LSB at frequencies around 220.3–220.7 GHz. We refer to Table 1 for their rest frequencies. A full astrochemical analysis of the data on CH_3CN (and other species) is beyond the scope of the present paper in which we concentrate on the spacial distributions of three lines of high and very high excitation, namely $k = 3/E_l = 122$ K, $k = 6/E_l = 315$ K, and $k = 9/E_l = 636$ K.

The full bandwidth of the SMA correlator is 4 GHz (2 GHz in each band). The SMA digital correlator was configured in to 24 spectral windows ("chunks") of 104 MHz each, with 256 channels distributed over each spectral window, thus providing a spectral resolution of 0.40 MHz (0.54 km s^{-1}) per channel. However, in this study we smoothed the spectral resolution to about 1 km s^{-1}.

The zenith opacity ($\tau_{230\ \rm GHz}$) was ∼0.1–0.3, indicating reasonable weather conditions. Observations of Uranus and Titan provided the absolute scale for the flux density calibration. Phase and amplitude calibrators were the quasars 0530+135, 0541-056, and 0607-085. The uncertainty in the flux scale is estimated to be 15–20%, based on the SMA monitoring of quasars. Further technical descriptions of the SMA and its calibration schemes can be found in Ho et al. (2004).

[1] The Submillimeter Array is a joint project between the Smithsonian Astrophysical Observatory and the Academia Sinica Institute of Astronomy and Astrophysics, and is funded by the Smithsonian Institution and the Academia Sinica.

The data were calibrated using the IDL superset MIR, originally developed for the Owens Valley Radio Observatory (Scoville et al. 1993) and adapted for the SMA[2]. The calibrated data were imaged and analyzed in a standard manner using the MIRIAD, GILDAS, and AIPS packages. We set the ROBUST parameter to 0 to obtain an optimal compromise between sensitivity and angular resolution. The line image rms noise was around 200 mJy beam^{-1} for each channel at an angular resolution of $3\farcs28 \times 3\farcs12$ with a PA = −14.0°.

2.2. Submillimeter

Data collected on 2003 December 12 were retrieved from the SMA archive. At the time of these observations, the SMA had seven antennas in its compact configuration with baselines ranging in projected length from 30 to 255 kλ. The primary beam of the SMA at 345 GHz has a *FWHM* of about 30″. The molecular emission from the hot core was found to be well inside the primary beam.

The receivers were tuned to a frequency of 347.33056 GHz in the upper sideband (USB), while the lower sideband (LSB) was centered on 337.33056 GHz. The LSB contained high excitation rotational lines from the first and second torsionally states of CH_3OH $\nu_t = 1$ and 2, respectively and from vibrationally excited states of HC_3N ($\nu_7 = 1$) and SO_2 ($\nu_2 = 1$); see Table 1 for their rest frequencies and lower level energies above the ground state, E_l. The SMA digital correlator was configured in to 24 spectral windows ("chunks") of 104 MHz each, with 128 channels distributed over each spectral window, thus providing a spectral resolution of 0.81 MHz (0.72 km s^{-1}) per channel. However, we smoothed the spectral resolution to 1.0 km s^{-1} per channel.

The zenith opacity ($\tau_{230\ \mathrm{GHz}}$) was ~0.035–0.04, indicative of excellent weather conditions. Observations of Uranus and Callisto provided the absolute scale for the flux density calibration. Phase and amplitude calibrators were the quasars 0420−014 and 3C 120. The uncertainty in the flux scale is also estimated to be 15–20%, based on the SMA monitoring of quasars.

The calibrated data were imaged and analyzed in a standard manner using the MIRIAD and AIPS packages. We used the ROBUST parameter set to 2 to achieve a slightly higher sensitivity while losing some angular resolution. The line image rms noise was around 170 mJy beam^{-1} for each channel at an angular resolution of $4\farcs2 \times 1\farcs30$ with a PA = −42.0°.

These archival data were previously presented in Beuther et al. (2005). However, we found important differences between our images of the vibrationally excited lines and the higher resolution images of that paper, which are discussed in more detail in the next section.

3. Results and discussion

3.1. Evidence of a close relation between the Orion KL hot core and the explosive disintegration event

We present evidence that the Orion KL hot core is no a typical hot core at all, with internal heating by a nascent star, but rather a condensation energized by the impact of high/low velocity material originating some 0.01 pc away in an external star-forming concentration.

Figure 1 shows an overlay of the H_2 "fingers" (Bally et al. 2010, in prep.), the blue- and red-shifted CO(2−1) filaments (Zapata et al. 2009), the integrated intensity distribution of the lower excitation CH_3CN (12_3–11_3) line, the positions of the three runaway stars (*BN*, *I* and *n*) and their dynamical center (Rodríguez et al. 2005; Gómez et al. 2005), and the submillimeter dust emission from the Orion KL region as mapped by the Submillimeter Common Bolometer Array (SCUBA) with the James-Clerk-Maxwell Telescope (Johnstone & Bally 1999). The intensity of the CH_3CN (12_3–11_3) line is integrated over the whole broad velocity range it covers, i.e. from −10 to +26 km s^{-1}. This thermal emission shows the classical heart-shaped morphology first revealed in 2″ resolution NH_3 images by Pauls et al. (1983) and later observed in many millimeter lines (see, e.g. Wilner et al. 1994). The heart is centered to the south of the dynamical origin of the three runaway stars and of the CO filaments, approximately in the middle between the positions of source *I* and *BN* (Zapata et al. 2009). The eastern lobe of the heart-shaped molecular structure shows a slight extension towards NNE with the same orientation as the highly obscured extended ridge as traced by the SCUBA observations. One clearly sees a correlation between the dark areas of the H_2 image and the submillimeter emission from the extended ridge, revealing the high extinction of this region.

Figure 1 shows that the northwest CO filaments are much clearly defined and longer than those located toward the southeast and southwest side of Orion KL, where the hot core is located. In addition, the H_2 fingers located in the northwest quadrant seem to be brighter and stronger than those found to the south. This suggests a possible relationship between the position of the Orion KL hot core and the absence of strong filaments in the described directions.

To gain additional insight into this relationship, we plot in Fig. 2 the distance from the explosive origin against the position angle on the sky of the CO(3−2) filaments discovered by Zapata et al. (in prep.). The CO(2−1) filaments found by Zapata et al. (2009) shown in their Fig. 1 are very similar to these but somewhat less well-defined. The diagram demonstrates how closely the absence of CO filamentary structures corresponds to the shadow area behind the hot core as observed in CH_3CN (12_3−11_3) emission. This suggests that the bulk of the high velocity CO gas accelerated by the explosion that traveling in these directions was stopped by a high density cloud (i.e. the extended ridge). The cloud was hereby heated, creating in the process the Orion KL hot core.

As mentioned above, the strong water maser emission observed toward the hot core region (Liu et al. 2002) displayed in Fig. 3 supports this picture, as probably does the OH maser emission. Interstellar OH masers exist mostly in the slowly (few km s^{-1}) expanding, warm (150 K), dense (10^{6-7} cm^{-3}) envelopes of ultracompact HII regions (Bloemhof et al. 1996; Fish et al. 2005), but weak ones have also been found, associated with the H_2O outflow from the W3OH TW object (Argon et al. 2003). We note that the total velocity spread of the Orion KL OH masers (≈55 km s^{-1}) is about 10 times larger than that found for a typical interstellar OH maser source (Cohen et al. 2006). The latter reference describes the idiosyncratic behavior of the emission in the different OH hyperfine transitions.

3.2. Distribution and kinematics of the molecular gas within the Orion KL hot core

3.2.1. Torsionally/vibrationally highly excited lines

In Fig. 3, we show the images of the distributions of four torsionally/vibrationally very highly excited lines, $CH_3OH(7_{4,3}$–$6_{4,3})$

[2] The MIR cookbook by C. Qi can be found at http://cfa-www.harvard.edu/~cqi/mircook.html

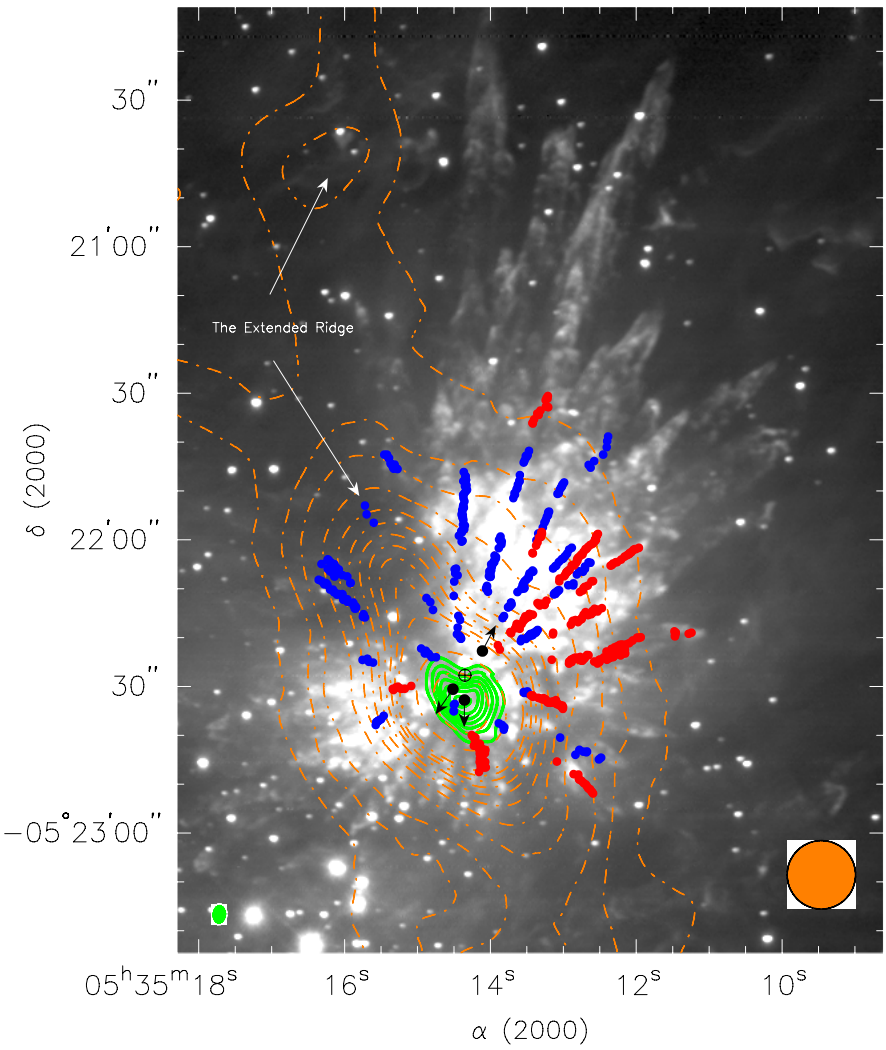

Fig. 1. H_2 image of the Orion KL region (Bally et al., in prep.) overlaid with an integrated intensity SMA map of $CH_3CN(12_3–11_3)$ (green contours), the positions of the blueshifted and redshifted CO(2−1) fingers from Zapata et al. (2009) (blue and red dots, respectively) and a SCUBA 850 μm continuum map from Johnstone & Bally (1999) (brown dashed contours). The green contours are −2, 2, 4, 6, 8, 10, 12, 14, 16, 18, and 20 times 30 Jy beam^{-1} km s^{-1}, the rms noise of the image. The brown dashed contours are −2, 2, 4, 6, 8, 10, 12, 14, 16, 18, and 20 times 3.5 Jy beam^{-1}. The black circles with vectors mark the positions and orientations of the proper motions of the radio and infrared sources *BN*, *I* and n (Rodríguez et al. 2005; Gómez et al. 2005). The black open circle with a cross represents the zone from where the three sources were ejected some 500 years ago, and the origin of the Orion KL molecular outflow as suggested by SMA CO(2−1) observations (Gómez et al. 2005; Zapata et al. 2009). The beam size of the SMA $CH_3CN(12_3–11_3)$ and the SCUBA maps are shown at the left- and right-hand bottom, respectively. The synthesized beam size of the SMA is 3.″28 × 3.″12 with a PA = −14.0°. The beam size of the SCUBA submillimeter observations is about 14″.

A^- (ν_t = 2), $CH_3OH(7_{4,3}–6_{4,3})$ A^- (ν_t = 1), $HC_3N(37–36)(\nu_7$ = 1), and $SO_2(21_{2,20}–21_{1,21})(\nu_2$ = 1), and the 870 μm continuum, overlaid on the moderate excitation CH_3CN $(12_3–11_3)$ line toward the core of the Orion KL region. These four lines have energies up to 943 K, thus trace the hottest molecular material. The continuum emission arises from only three compact sources that were already reported at millimeter wavelengths by Blake et al. (1996); Wright et al. (1996); Plambeck et al. (1995); namely the hot core -> SMM3, the northwest clump -> SMM2, and the compact ridge -> SMM1. In Table 2, we list their observational parameters. The source SMM1 is further resolved into three compact sources: SMA 1, hot core, and source *I* (Beuther et al. 2004). The 1300 μm continuum emission is quite similar to that at 870 μm, so we do not show a map at this wavelength.

The torsionally/vibrationally highly excited emission is seen to be compact and located exclusively on the northeast side of the heart-shaped structure as traced by the emission of $CH_3CN(12_3–11_3)$. We list the observational and physical parameters of these lines in Table 1. The CH_3OH and HC_3N emission clearly shows pronounced extensions or tails toward the northeast part of the hot core, oriented in the direction of the extended ridge. A similar tail or extension is also observed in $CH_3CN(12_3–11_3)$. The $HC_3N(37–36)(\nu_7$ = 1) and $CH_3OH(7_{4,3}–6_{4,3})$ A^- (ν_t = 2) line emissions seem to surround the submillimeter source SMM3 like part of a shell, and both lines peak between the submillimeter source and the origin of the explosion. The morphology of the $HC_3N(37–36)(\nu_7$ = 1) emission even appears to point toward the origin. The vibrationally excited SO_2 emission, with an energy of the lower state of almost 1000 K (see Table 1), is very compact and peaks at the same position as the $HC_3N(37–36)(\nu_7$ = 1) emission.

We note that the vibrationally/torsionally excited lines are not associated with any radio or submillimeter continuum sources and always fall well outside or on the edge of the

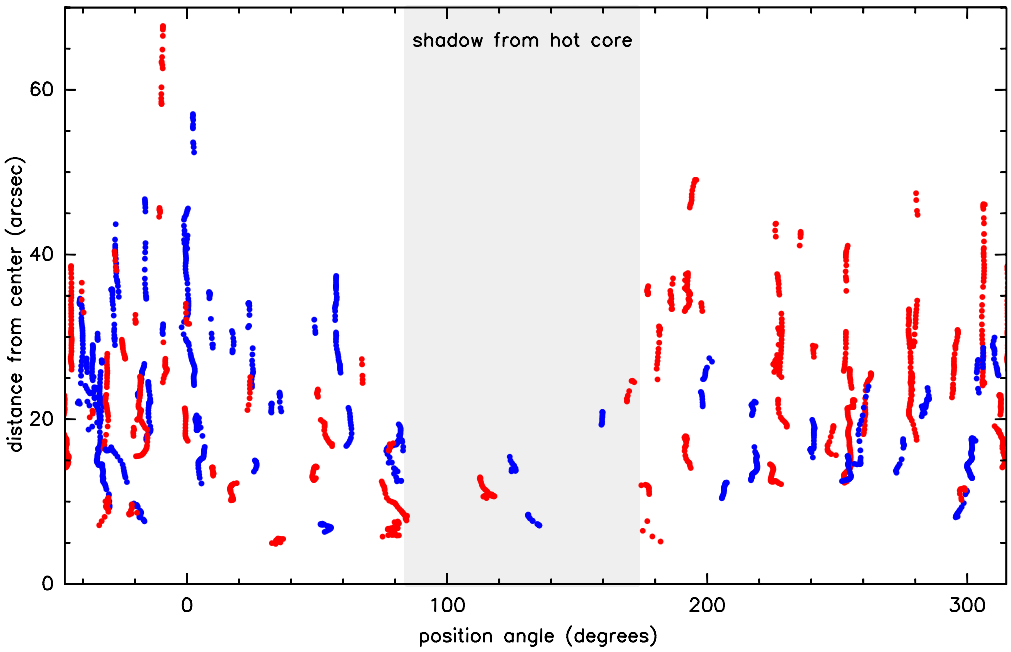

Fig. 2. Distance from the explosion origin or center vs. position angle on the sky of the CO(3−2) molecular filaments obtained by Zapata et al. (in prep.). The explosive origin is located in α[2000] = $0^h35^m14.37^s$ and δ[2000] = $-05°22'27.9''$. The light grey area marks the "shadow" caused by the Orion KL hot core; filaments are prevented by the hot core from expanding into this sector. The blue filaments indicate the CO(3−2) molecular gas approaching towards us, while red ones are those receding.

Table 2. Observational parameters of the submillimeter and millimeter compact sources.

			870 μm		1300 μm		
	RA	Dec	Flux density	Peak flux	Flux density	Peak flux	Spectral
Sources	J[2000]	J[2000]	[Jy]	[Jy Beam^{-1}]	[Jy]	[Jy Beam^{-1}]	Index[a]
SMM1	5 35 14.015	−5 22 36.88	4.0	1.5	1.3	0.7	2.9
SMM2	5 35 14.087	−5 22 27.55	5.6	2.6	1.5	0.7	3.3
SMM3	5 35 14.560	−5 22 31.38	11.1	4.2	4.8	2.7	2.1

Notes. [(a)] The beam size of the two measurements is quite similar, thus *warranting* that we are sensitive to the same spatial scales.

heart-shaped structure traced by $CH_3CN(12_3–11_3)$ (see Fig. 3). This suggests that the heating source of the hot core is external as proposed by Blake et al. (1996) and Liu et al. (2002).

If the heating of the Orion KL hot core were internal, one might expect the hot molecular gas to be centered on a strong compact continuum source located within the core, but this is not the case. Both $HC_3N(37–36)(v_7 = 1)$ and $CH_3OH(7_{4,3}–6_{4,3})$ A^- $(v_t = 2)$ seem to form a shell around the continuum source Hot Core speaks against any internal heating scenario, being indicative instead of heating coming from outside.

The torsionally/vibrationally highly excited lines are exclusively placed along the densest and most highly obscured parts of Orion KL, i.e. on the extended ridge. We do not find any such emission associated with the compact ridge or the northwest clump. This is in very good agreement with the observations of vibrationally excited HC_3N (Blake et al. 1996; Wright et al. 1996; de Vicente et al. 2002). However, comparison of our submillimeter line maps with those of millimeter wavelengths indicates that the hottest molecular gas is located only in the northwest part of the millimeter/submillimeter source SMM3.

The high angular resolution maps ($\leq 1''$) presented in Beuther et al. (2005) differ considerably from ours, as well as from the vibrationally excited line emission presented by Blake et al. (1996); Wright et al. (1996); de Vicente et al. (2002) at millimeter wavelengths. To understand these differences between the SMA maps, we recalibrated the high angular resolution data of Beuther et al. which is a factor of more than four better than our actual resolution, and made some images of their vibrationally/torsionally excited lines. In all these maps, we found pronounced negative and positive sidelobe structures going from west to east, with most of the compact positive structures showing nearly random behavior that prohibits us from determining which of these compact sources are real. This suggests that part of the emission here must have been resolved out.

3.2.2. Emission of $CH_3CN(12–11)$ in the vibrational ground state

In Fig. 4, we show a SMA $CH_3CN(12_k–11_k)$ color composite of the rotational transitions $k = 9$, $k = 6$, and $k = 3$ overlaid on the $HC_3N(37–36)(v_7 = 1)$ and $SO_2(21_{2,20}–21_{1,21})(v_2 = 1)$ integrated line emissions. The image reveals that $CH_3CN(12_9–11_9)$, which is supposed to trace the positions of very hot molecular gas (see Table 1), is also located in the northeast part of the heart-shaped structure where all the torsionally/vibrationally excited lines are found. This confirms that the hottest molecular gas is found in this part of the Orion KL hot core. However, there is a clear offset (toward the southeast) between the vibrationally/torsionally excited lines and this ground state line. The $CH_3CN(12_3–11_3)$ emission, on the other hand, reveals that the coldest part of the molecular heart-shaped structure is located toward the compact ridge.

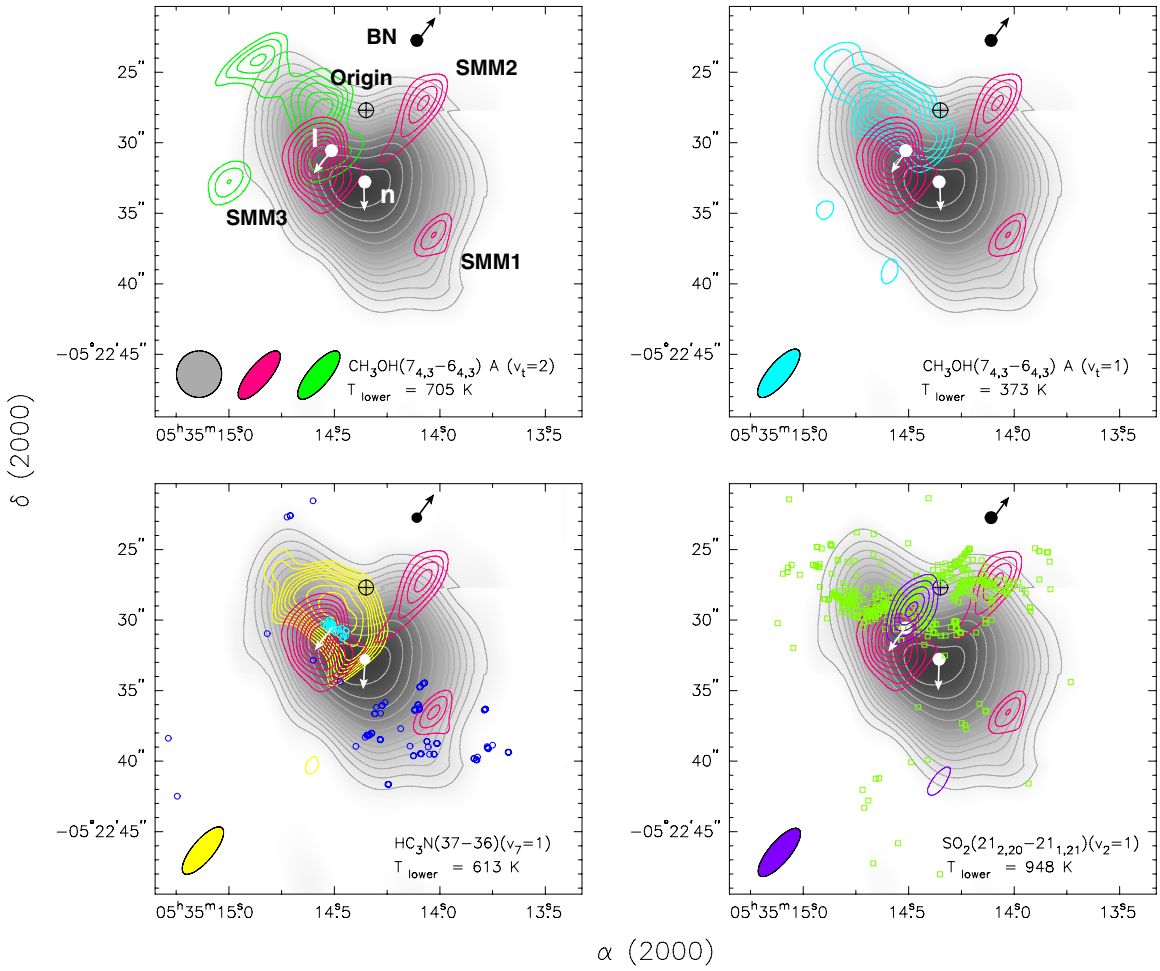

Fig. 3. Overlays of the SMA 870 μm continuum map (pink contours) and the integrated line emission maps of four submillimeter tosionally/vibrationally excited lines towards the Orion *BN*-KL region onto the $CH_3CN(12_3–11_3)$ integrated line emission map (grey). The pink contours are from 40% to 90% with steps of 5% the peak of the continuum emission, 4.5 Jy beam^{-1}. The grey contours are −2, 2, 3, 4, 5, 6, 7, 8, 9, 10, 12, 14, 16, 18, and 20 times 30 Jy beam^{-1} km s^{-1}, the rms noise of the image. *Upper left panel*: $CH_3OH(7_{4,3}–6_{4,3})$ A$^-$ (ν_t = 2): green contours. The contours are from 35% to 90% with steps of 10% of the peak of the line emission, 37 Jy beam^{-1} km s^{-1}. *Upper right panel*: $CH_3OH(7_{4,3}–6_{4,3})$ A$^-$ (ν_t = 1) (blue contours). The contours are from 35% to 90% with steps of 10% of the peak of the line emission, 50 Jy beam^{-1} km s^{-1}. *Lower left panel*: $HC_3N(37–36)(\nu_7 = 1)$ (yellow contours). The contours are from 20% to 90% with steps of 10% the peak of the line emission, 170 Jy beam^{-1} km s^{-1}. *Lower right panel*: $SO_2(21_{2,20}–21_{1,21})(\nu_2 = 1)$ (purple contours). The contours are from 40% to 90% with steps of 5% the peak of the integrated emission, 35.1 Jy beam^{-1} km s^{-1}. In every panel, the black and white circles with vectors mark the position and the orientation of the proper motions of the radio and infrared sources *BN*, *I*, and *n*. The black open circle with a cross represents the zone from which the three sources were ejected some 500 years ago and that is the origin of the Orion-KL molecular outflow as suggested by the SMA CO(2−1) observations. The synthesized beams of the SMA millimeter and submillimeter observations are shown in the bottom left hand part of each panel. The blue open circles and green squares mark the positions of the H_2O and OH maser spots, respectively (Gaume et al. 1998; Cohen et al. 2006). The light blue open circles show the water masers close to source *I*.

All the emission peaks of these lines, ($CH_3CN(12_9–11_9)$, $SO_2(21_{2,20}–21_{1,21})(\nu_2 = 1)$, and $HC_3N(37–36)(\nu_7 = 1)$), are well concentrated in the southeast sector of the filamentary CO structure and aligned with the band of highest $HC_3N(37–36)(\nu_7 = 1)$ line width (Fig. 5).

We note that the ground-state line $CH_3CN(12_9–11_9)$ is not coincident with any of the submillimeter or radio continuum sources located in this region.

3.2.3. Kinematics

We show the kinematics of the molecular gas within the hot core and the compact ridge regions in Fig. 5, where moment one (integrated weighted velocity) and two (integrated velocity dispersion squared) maps of the vibrationally excited ground-state emission from the $CH_3CN(12_3–11_3)$ and $HC_3N(37–36)(\nu_7 = 1)$ lines, respectively are displayed. The moment one maps show that the blueshifted molecular gas is concentrated in the northeast part of the heart-shaped structure, while the redshifted gas is located on the northwest part. The origin of the runaway stars and the filamentary structure is well placed in between, in the middle of the northern lobes of the heart-shaped structure defined by $CH_3CN(12_3–11_3)$. The emission of $HC_3N(37–36)(\nu_7 = 1)$ is entirely blueshifted with a respect to ambient and shows a velocity gradient with northeast-southwest orientation.

The moment two maps appear to reveal filamentary structures. These "filaments" seem to be reminiscent of the filamentary CO(2−1) emission found by Zapata et al. (2009). However, from this image it is also clear that the largest line widths are located at the center of the heart-shaped core and smaller at the edge implying that the source of the shocks could be inside the "hot core".

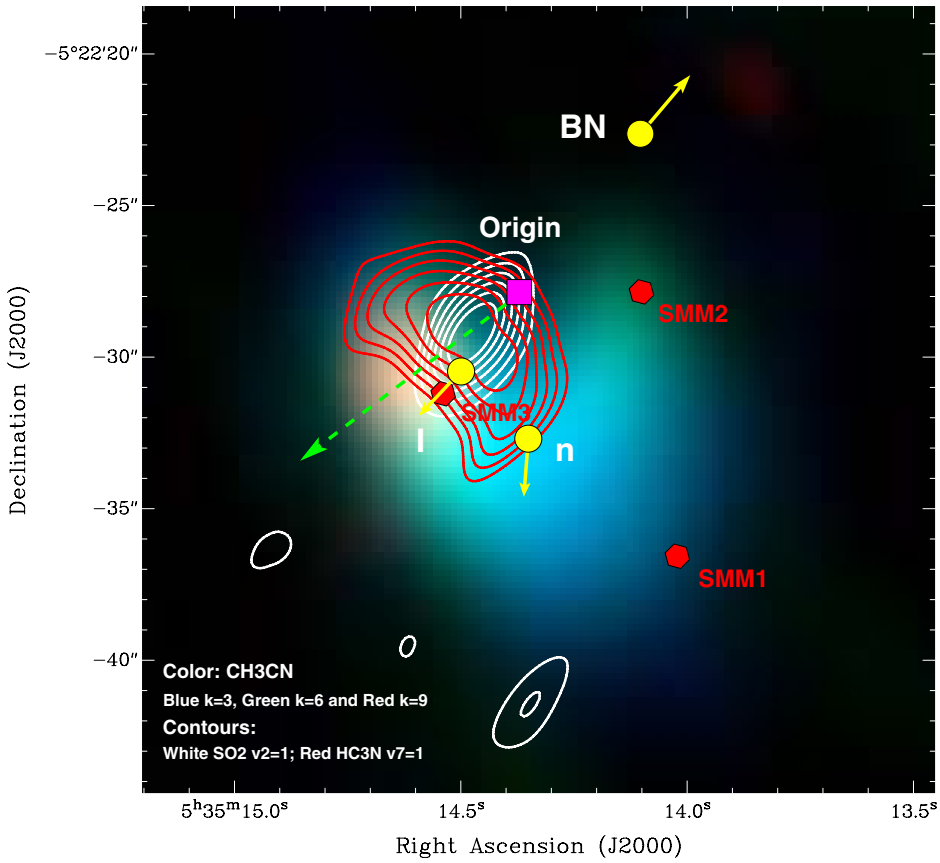

Fig. 4. SMA $CH_3CN(12_k–11_k)$ composite image with red representing the rotational transition $k = 9$, green $k = 6$, and blue $k = 3$. Overlaid on this image are $HC_3N(37–36)(v_7 = 1)$ and $SO_2(21_{2,20}–21_{1,21})(v_2 = 1)$ integrated emissions (red and white contours, respectively). The red contours are from 30% to 90% with steps of 12% of the peak of the line emission (170 Jy beam^{-1} km s^{-1}). The integrated velocity range of the $HC_3N(37–36)(v_7 = 1)$ line emission is from −12 to +19 km s^{-1}. The white contours are from 40% to 90% with steps of 5% of the peak of the integrated emission (35.1 Jy beam^{-1} km s^{-1}). The integrated velocity range of the $SO_2(21_{2,20}–21_{1,21})(v_2 = 1)$ line emission is from −1 to +13 km s^{-1}. The yellow circles with vectors mark the same positions as in Figs. 3 and 4, the pink square represents the origin of the Orion KL molecular outflow as suggested by our SMA CO(2−1) observations. The red hexagons mark the positions of the three submillimeter sources SMM1, SMM2, and SMM3, the green dashed arrow the position and orientation of the filament structure revealed by the moment two map of $HC_3N(37–36)(v_7 = 1)$, see Fig. 5.

We propose that the −4 km s^{-1} blueshifted component found in $HC_3N(37–36)(v_7 = 1)$ and $CH_3OH(7_{4,3}–6_{4,3})$ is perhaps excited by one filament that collided with a slightly different velocity toward this position.

3.3. The relation between the centimeter, submillimeter, infrared, and molecular line emission

A superimposition of the $HC_3N(37–36)(v_7 = 1)$, $CH_3OH(7_{4,3}–6_{4,3})$ A^- $(v_t = 2)$, and submillimeter continuum emission on the 11.7 μm infrared emission detected by Smith et al. (2005) from the Orion KL region is displayed in Fig. 6. In this image, we included the positions of the four radio sources *BN*, *I*, *n*, and *D* (Zapata et al. 2004; Gómez et al. 2005; Rodríguez et al. 2009). The map shows a lack of correspondence between the centimeter, submillimeter, and mid-infrared continuum sources. This poor coincidence suggests that they might have a different nature. We found three groups of similar sources in the Orion KL region, which we describe as follows:

– the first group is formed by the compact millimeter and submillimeter sources SMM1, SMM2, and SMM3. These sources seem to be deeply embedded in the Orion Molecular Cloud, with no strong mid-/near-infrared nor centimeter emission. They appear to be optically thick, dusty compact objects as suggested by their large positive spectral indices (see Table 2). As revealed by our observations, they do not show hot core activity;
– a second group consists of the infrared and centimeter sources *BN*, *I*, and *n*. These sources have only very faint mm or submm emission associated with them and do not show any of the hot molecular emission typically characterizing hot cores;
– a third group is formed by the extended infrared sources with vibrationally/torsionally excited molecular emission. This emission is related only to the infrared objects IRS2a-d (Dougados et al. 1993; Gezari et al. 1998). This type of source does not have any centimeter or submillimeter counterparts, suggesting that it is not be self-luminous, as first proposed by Menten & Reid (1995). This thermal infrared and molecular emission was created possibly by shocks from the explosive disintegration of the stellar system.

Since the mid-infrared image shows a good correspondence with the hot molecular gas traced by the vibrationally/torsionally excited emission, the mid-infrared emission is not necessarily be reprocessed emission escaping through inhomogeneities in the dense material but might be due to heating by a shock compression that destroyed the dust grains.

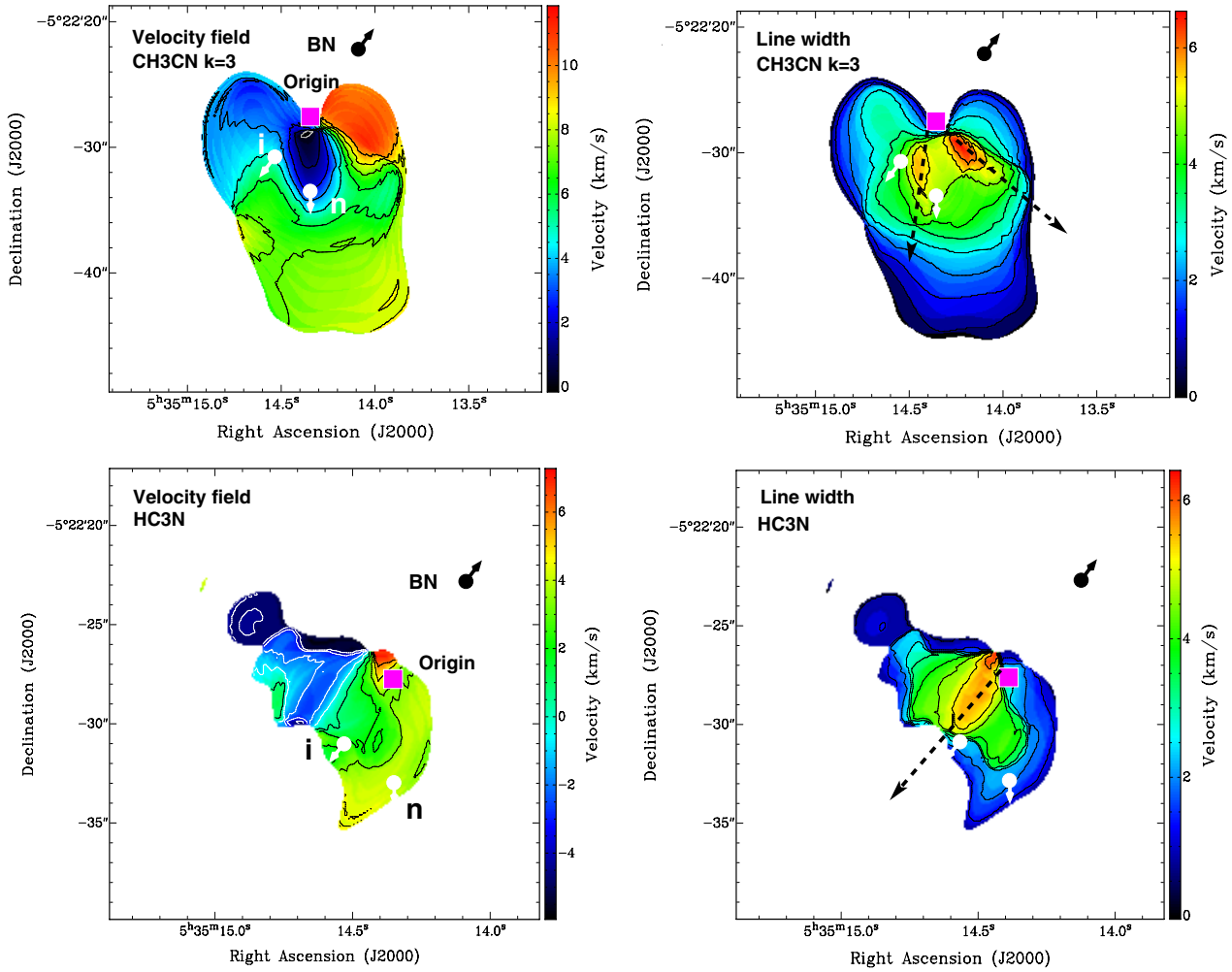

Fig. 5. SMA moment one and two color scale maps of the emission of $CH_3CN(12_3–11_3)$ (*upper* images) and $HC_3N(37–36)(v_7 = 1)$ (*lower* images), respectively. The black and white circles are as in Fig. 3. The violet square represents the origin of the CO(2−1) filaments (Zapata et al. 2009). The arrows mark the position and orientation of the putative filaments.

Vibrationally/torsionally excited lines might be only observed towards IRS2 because only this spot has a density or temperature high enough to ensure sufficient excitation. In Fig. 1 one can see that towards the position of this emission the highly extincted and dense extended ridge is located. Molecular lines that trace colder gas, such as $NH_3(4, 4)$, are not present at the locations of the mid-infrared and vibrationally/torsionally excited molecular emission (Fig. 5 of Cohen et al. 2006).

We note that the submillimeter source "compact ridge" (SMM1) seems to be surrounded by mid-infrared emission oriented in approximately the direction of the dynamical origin but any associated hot molecular gas.

It is interesting to mention that most of the eastern OH maser spots mapped by Cohen et al. (2006) show good coincidence with the vibrationally/torsionally excited emission reported here. Moreover, part of the OH maser emission seems to cover the submillimeter source SMM3 in a similar way the vibrationally/torsionally excited emission. This argues in favor of the infrared emission being produced by shocks.

3.4. What is source *I*?

The presence and peculiar properties of radio source *I* add substantially to the complexity of the KL region's appearance. One might assume that the molecular outflow from *I* (Plambeck et al. 2009) heats the Orion KL hot core because it lies along the same orientation as the vibrationally/torsionally excited lines. However, if this were the case one would expect the largest linewidths in the moment two maps (Fig. 5) to be found at the position of source *I*, something that is not observed.

This wide angle flow from *I*, whose origin is possibly an expanding, rotating thick disk traced by SiO maser emission (Matthews et al. 2010), does not appear to be dynamically coupled to any other phenomenon in the KL region. The observed radio emission from *I* is consistent with an early type B star (B0–B1) ionizing the inner regions of the disk (Reid et al. 2007).

As discussed by Bally & Zinnecker (2005), wide angle outflows – expanding disks – are a natural consequence of stellar mergers. A merger of a 20 $M_\odot$ star swallowing a 1 $M_\odot$ object will release about 3×10^{48} erg of potential energy, more than that required to power the KL region. This line of argument is consistent with source *I* being the end result of a merger. The reason for *BN*, *n*, and *I* all moving away from each other after the merger event should be investigated by numerical simulations.

It is difficult to estimate a precise dissipation timescale of the energy released on the dynamical non-hierarchical disintegration. However, if the central "hole" found on the CO filaments (Zapata et al. 2009) were generated because of the cooling of

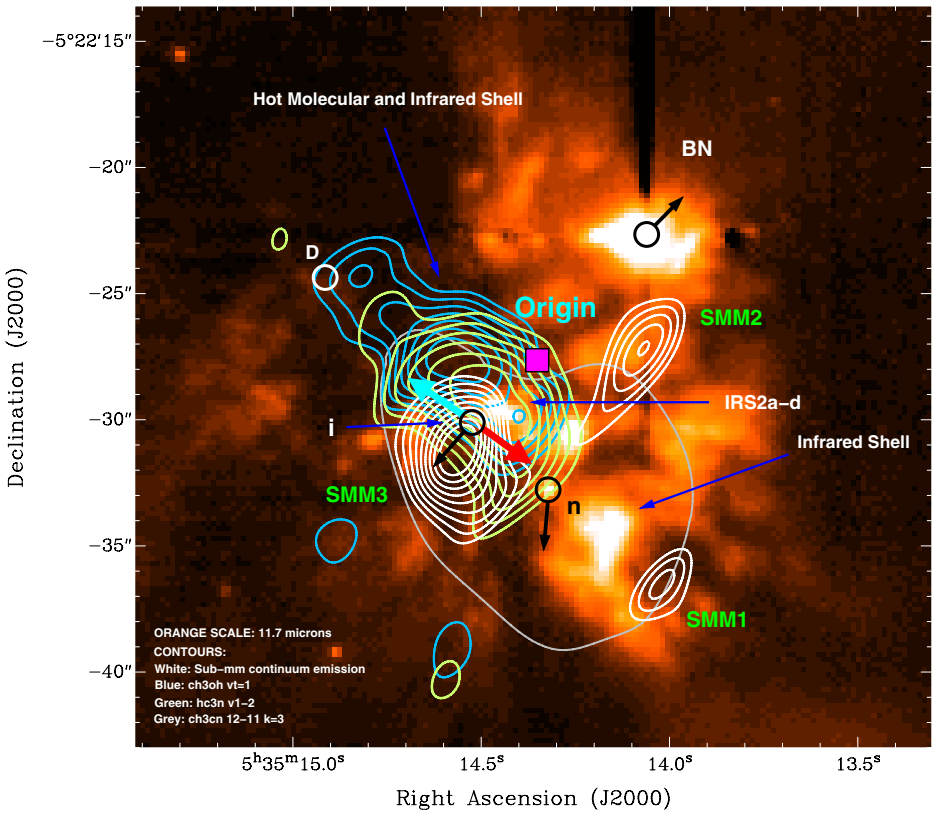

Fig. 6. Gemini 11.7 μm continuum image (orange) from Smith et al. (2005) overlaid with SMA maps of the submillimeter continuum emission (faint white contours), the $CH_3OH(7_{4,3}–6_{4,3})$ A^- (ν_t = 1) and $HC_3N(37–36)(\nu_7$ = 1) integrated emission (blue and green contours, respectively) and the rotational integrated emission of $CH_3CN(12_3–11_3)$ (single grey contour) toward the Orion KL region. The white contours are from 40% to 90% with steps of 5% of the peak of the continuum emission (4.5 Jy beam^{-1}). The blue contours are from 30% to 90% with steps of 10% of the peak of the line emission, 37 Jy beam^{-1} km s^{-1}. The integrated velocity range of the $CH_3OH(7_{4,3}–6_{4,3})$ A^- (ν_t = 2) is from −5 to +15 km s^{-1}. The green contours are from 25% to 90% with steps of 12% of the peak of the line emission (170 Jy beam^{-1} km s^{-1}). The integrated velocity range of $HC_3N(37–36)(\nu_7$ = 1) is from −12 to +19 km s^{-1}. The single grey contour is 34% of the peak of the line emission (586 Jy beam^{-1} km s^{-1}). The integrated velocity range of $CH_3CN(12_3–11_3)$ is from −10 to +26 km s^{-1}. Black circles and pink square as in previous figures. The blue and red arrows at the position of source *I* show the approximate orientation of the thermal and SiO maser outflow emanating from this object (Plambeck et al. 2009; Matthews et al. 2010). The white open circle marks the position of the radio source *D* (Zapata et al. 2004; Gómez et al. 2005).

the molecular gas on the outflow, the time of dissipation for the outflow would be on the order of five thousand years.

3.5. Heating of the Orion KL hot core by an explosive flow

Since we do not find hot molecular gas emission to be associated with any self-luminous submillimeter, radio, or infrared source, and this emission is restricted to the northeast edge of the heart-shaped structure, the heating source of the Orion KL hot core might be external. Since $HC_3N(37–36)(\nu_7$ = 1) and $CH_3OH(7_{4,3}–6_{4,3})$ A^- (ν_t = 1) seem to form part of a shell around the submillimeter source SMM3, and this shell points in the direction of the dynamical center, the heating source seems to be closely linked to that center.

Furthermore, the unique absence of CO filamentary flow structures or "fingers" from the area behind the Orion KL hot core (i.e. behind relative to the outflow center) indicates that a dense zone of the extended ridge might have impeded the expansion of these filaments.

It is important to realize that each individual CO filament obeyed a Hubble-type velocity, i.e. its velocity increases linearly with distance from the explosive origin (Zapata et al. 2009), in other words, during the explosive event some 500 years ago material of vastly different velocities was ejected simultaneously and has traveled to different distances and locations. The material that has just arrived at the hot core condensation is the one that now excites the energetic vibrations observed. We do not, therefore, require decay times of this shock excitation to be on the order of hundreds of years; the emission we observe now is instead caused by streams of matter impinging at present, not in the "distant" past (~500 years), hence the relevant decay times may be indeed very much shorter. One can roughly estimate the cooling or decay time for the molecular gas. The cooling time goes as $nkT/\lambda(T)$, where $\lambda(T)$ is the cooling rate is given by about $1 \times 10^{-27}\ T^{0.4}$ (cm^3 erg s^{-1}) for the temperatures range between 100–10^4 K (McKee & Cowie 1977), n is the density in cm^{-3}, k is Boltzmann constant, and T is the temperature in Kelvin. Assuming a temperature of 200 K and a density of $10^{4–6}$ cm^{-3} for the Orion "hot core" (Kaufman et al. 1998), we found a cooling time <100 years, which is indeed very short.

Kaufman et al. (1998) argued that the Orion KL hot core is more likely to be heated by stars embedded within the core than powered from outside because of the core's large column densities, and warm temperatures. However, these large column densities and warm temperatures could be generated by fast and energetic shocks arriving now at the core as discussed above. Thus it is not necessary to have an internal warm stellar source for heating the Orion-KL hot core.

Here, "external heating" has a different sense to that discussed and proposed by Kaufman et al. (1998), i.e. the dense core in Orion-KL (such as the extended ridge) was heated from outside by the impact of one or multiple low-velocity shock waves from the explosive event thus creating the "hot core". This means that the core is not heated by young stars either outside or inside the dense core.

From the internally heated hot core picture, one may then expect to find the hottest molecular gas associated with the central massive protostellar source where the high temperatures and column density reside and can excite these molecules. This is not, however, the case for the Orion KL hot core. We found that none of the hot molecular tracers presented here are associated with a self-luminous source. Moreover, the hot gas is found at an edge of the region traced by cold and/or warm gas from other molecules (e.g. the $CH_3CN(12_3–11_3)$), which is strongly suggestive of external heating. The molecular emission with low excitation temperatures and/or critical densities may have a very erratic behavior for different species, and be unhelpful in pinpointing the true exciting source as already observed in the Orion KL hot core (Wilson et al. 2000; Blake et al. 1996; Wright et al. 1996), and in some other hot cores (Brogan et al. 2007; Mookerjea et al. 2007).

3.6. Consequences of KL not being a typical hot core

In principle, there should be observable differences between the KL region and a typical hot molecular core. For one, the chemistry in KL should be shock driven with much higher temperatures than the chemistry in a typical hot core. In typical cores, heating the dust grains to just about a hundred K is sufficient to evaporate complex molecules from their grain surfaces, and producing the high observed abundances of organics, which can be orders of magnitude higher than in cold molecular cloud material (see, e.g., van der Tak et al. 2000; Herbst & van Dishoeck 2009).

Strong shocks that evaporate the dust grains, causing many molecules into the gas phase, could be more efficiently generated by low-velocity (~50 km s^{-1}) C-shock mediated grain-sputtering, which seems to be more effective that grain-grain collisions or even J-shocks (Flower & Pineau des Forets 1995; May et al. 2000).

In a fast shock similar to the one driven by the explosive event in the KL region most molecules are probably dissociated. Detailed models of the ensuing chemical evolution at these much higher temperatures do not exist at present. In particular, it is unknown to what stage the evolution can proceed on the short time scale involved, some 500 years.

Another relevant finding is the missing class II methanol maser in KL. Toward many hot cores associated with high mass protostars, maser emission in the strongest class II maser line at 6.7 GHz is observed, *a.o.*, in Orion S (Voronkov et al. 2005). However, toward the KL region these authors only find a feature whose line width, strength, and distribution is consistent with the values found for thermal (non-maser) emission from numerous other molecular lines. The presence of a class II methanol maser is a sufficient, but not unnecessary condition for a source to be a hot core; it is indeed remains unclear what percentage of hot cores host such a maser, although probably most do (Ellingsen 2006). We find the absence of such a maser from the KL region to be remarkable.

In contrast, about a dozen compact regions exhibiting strong maser emission in the 25 GHz maser lines, which corresponds to classical class I methanol maser transitions, are distributed throughout over the KL region. Whether or not these masers have any relation to the explosive event (or to any other phenomenon in the region) is presently completely unclear.

4. Conclusions

We have observed and analyzed the submillimeter and millimeter torsionally/vibrationally highly excited lines $CH_3OH(7_{4,3}–6_{4,3})$ A$^-$ (ν_t = 2), $CH_3OH(7_{4,3}–6_{4,3})$ A$^-$ (ν_t = 1), $HC_3N(37–36)$ (ν_7 = 1), $SO_2(21_{2,20}–21_{1,21})(\nu_2$ = 1), as well as $CH_3CN(12_k–11_k)$ with k = 3, 6, 9 and the continuum emissions at 870 and 1300 μm, from the Orion KL region in an attempt to clarify the nature of the "hot molecular core" located in this region. Our main findings are as follows:

- The system of high velocity CO filaments or "fingers" that is believed to have originated in an explosive stellar merger event some 500 years ago is being blocked in its southwest quadrant by the intervening Orion KL hot core. The area behind the hot core is uniquely devoid of such filaments. An H_2 image of the region likewise shows the northwestern fingers to be much stronger and better defined than southern ones.
- The low excitation $CH_3CN(12_3–11_3)$ emission shows the typical heart-shaped structure mapped in many molecules; indentation of the heart-shaped structure is centered close to the dynamical origin of the explosion.
- The torsionally/vibrationally excited lines and $CH_3CN(12_9–11_9)$, all of which are supposed to trace hot and dense molecular gas, are located exclusively toward the northeast lobe of the heart-shaped structure, i.e. toward the densest and most highly obscured parts of the extended ridge. The $HC_3N(37–36)(\nu_7$ = 1) and $CH_3OH(7_{4,3}–6_{3,3})$ A$^-$ (ν_t = 1) lines appear to form a shell around the strongest compact submillimeter source, SMM3, and to point toward the dynamical origin of the CO filaments.
- The $CH_3CN(12_3–11_3)$ and $HC_3N(37–36)(\nu_7$ = 1) maps of the kinematics of the molecular gas within the hot core appear to reveal filament-like structures. The peculiar turbulent velocity field of the Orion KL hot core is possibly the result of gas moving in different directions because of the explosive event.
- The peaks of the emission from $CH_3CN(12_9–11_9)$, $SO_2(21_{2,20}–21_{1,21})(\nu_2$ = 1), and $HC_3N(37–36)(\nu_7$ = 1) are all strongly concentrated in the southeast filamentary structure given by the moment two maps. This suggests a close relationship between the excitation of these three lines and the filamentary structure.
- Only three compact submillimeter sources that are counterparts of millimeter sources previously reported in the literature, SMM1, SMM2, and SMM3, could be found. All three sources have steep spectral indices indicative of optically thick dust emission.
- The hottest molecular emission coincides well with a chain of mid-infrared (IRS2a-d) and OH maser emissions, suggesting that part of the infrared emission of the Orion KL region might be generated by strong shocks.
- There are at least three types of objects in the Orion KL region: The radio continuum sources with or without infrared emission and no hot core activity (*BN*, *n*, and *I*) that formed a stellar group in the past; the submillimeter sources with neither mid-infrared emission nor any hot core activity (SMM1, SMM2, and SMM3); and the extended mid-infrared continuum emission with or without associated molecular emission that is probably generated by strong shocks.

The various millimeter and submillimeter SMA observations suggest that the Orion KL hot core is heated by the explosive flow associated with the disintegration of a massive young stellar system. This hypothesis can explain most of the peculiar features observed in the Orion KL hot core such as its strange velocity fields and peculiar morphology. However, additional theoretical and observational studies are required to test this new heating scenario.

Acknowledgements. We are very grateful to Nathan Smith and John Bally for having provided the 11.7 μm infrared and the H_2 images. We would like also to thank to the anonymous referee and Malcolm Walmsley for the detail comments and suggestions to improve this study.

References

Argon, A. L., Reid, M. J., & Menten, K. M. 2003, ApJ, 593, 925
Bally, J., & Zinnecker, H. 2005, AJ, 129, 2281
Beuther, H., Zhang, Q., Greenhill, L. J., et al. 2004, ApJ, 616, L31
Beuther, H., Zhang, Q., Greenhill, L. J., et al. 2005, ApJ, 632, 355
Blake, G. A., Mundy, L. G., Carlstrom, J. E., et al. 1996, ApJ, 472, L49
Bloemhof, E. E., Moran, J. M., & Reid, M. J. 1996, ApJ, 467, L117
Bottinelli, S., Ceccarelli, C., Neri, R., et al. 2004, ApJ, 617, L69
Brogan, C. L., Chandler, C. J., Hunter, T. R., Shirley, Y. L., & Sarma, A. P. 2007, ApJ, 660, L133
Ceccarelli, C., Loinard, L., Castets, A., Tielens, A. G. G. M., & Caux, E. 2000, A&A, 357, L9
Cesaroni, R. 2005, in Massive Star Birth: A Crossroads of Astrophysics, ed. R. Cesaroni, M. Felli, E. Churchwell, & M. Walmsley, IAU Symp., 227, 59
Chandler, C. J., & Wood, D. O. S. 1997, MNRAS, 287, 445
Chernin, L. M., & Wright, M. C. H. 1996, ApJ, 467, 676
Cohen, R. J., Gasiprong, N., Meaburn, J., & Graham, M. F. 2006, MNRAS, 367, 541
de Vicente, P., Martín-Pintado, J., Neri, R., & Rodríguez-Franco, A. 2002, ApJ, 574, L163
Dougados, C., Lena, P., Ridgway, S. T., Christou, J. C., & Probst, R. G. 1993, ApJ, 406, 112
Ellingsen, S. P. 2006, ApJ, 638, 241
Fish, V. L., Reid, M. J., Argon, A. L., & Zheng, X. 2005, ApJS, 160, 220
Flower, D. R., & Pineau des Forets, G. 1995, MNRAS, 275, 1049
Friedel, D. N., & Snyder, L. E. 2008, ApJ, 672, 962
Gaume, R. A., Wilson, T. L., Vrba, F. J., Johnston, K. J., & Schmid-Burgk, J. 1998, ApJ, 493, 940
Genzel, R., & Stutzki, J. 1989, ARA&A, 27, 41
Genzel, R., Reid, M. J., Moran, J. M., & Downes, D. 1981, ApJ, 244, 884
Genzel, R., Ho, P. T. P., Bieging, J., & Downes, D. 1982, ApJ, 259, L103
Gezari, D. Y., Backman, D. E., & Werner, M. W. 1998, ApJ, 509, 283
Gómez, L., Rodríguez, L. F., Loinard, L., et al. 2005, ApJ, 635, 1166
Herbst, E., & van Dishoeck, E. F. 2009, ARA&A, 47, 427
Ho, P. T. P., Barrett, A. H., Myers, P. C., et al. 1979, ApJ, 234, 912
Ho, P. T. P., Moran, J. M., & Lo, K. Y. 2004, ApJ, 616, L1
Johnstone, D., & Bally, J. 1999, ApJ, 510, L49
Kaufman, M. J., Hollenbach, D. J., & Tielens, A. G. G. M. 1998, ApJ, 497, 276
Kurtz, S., Cesaroni, R., Churchwell, E., Hofner, P., & Walmsley, C. M. 2000, Protostars and Planets IV, 299
Liu, S., Girart, J. M., Remijan, A., & Snyder, L. E. 2002, ApJ, 576, 255
Masson, C. R., & Mundy, L. G. 1988, ApJ, 324, 538
Matthews, L. D., Greenhill, L. J., Goddi, C., et al. 2010, ApJ, 708, 80
Mauersberger, R., Wilson, T. L., & Walmsley, C. M. 1986, A&A, 166, L26
May, P. W., Pineau des Forêts, G., Flower, D. R., et al. 2000, MNRAS, 318, 809
McKee, C. F., & Cowie, L. L. 1977, ApJ, 215, 213
Menten, K. M., & Reid, M. J. 1995, ApJ, 445, L157
Menten, K. M., Reid, M. J., Forbrich, J., & Brunthaler, A. 2007, A&A, 474, 515
Migenes, V., Johnston, K. J., Pauls, T. A., & Wilson, T. L. 1989, ApJ, 347, 294
Mookerjea, B., Casper, E., Mundy, L. G., & Looney, L. W. 2007, ApJ, 659, 447
Pauls, A., Wilson, T. L., Bieging, J. H., & Martin, R. N. 1983, A&A, 124, 23
Plambeck, R. L., Wright, M. C. H., Mundy, L. G., & Looney, L. W. 1995, ApJ, 455, L189+
Plambeck, R. L., Wright, M. C. H., Friedel, D. N., et al. 2009, ApJ, 704, L25
Reid, M. J., Menten, K. M., Greenhill, L. J., & Chandler, C. J. 2007, ApJ, 664, 950
Rodríguez, L. F., Poveda, A., Lizano, S., & Allen, C. 2005, ApJ, 627, L65
Rodríguez, L. F., Zapata, L. A., & Ho, P. T. P. 2009, ApJ, 692, 162
Scoville, N. Z., Carlstrom, J. E., Chandler, C. J., et al. 1993, PASP, 105, 1482
Smith, N., Bally, J., Shuping, R. Y., Morris, M., & Kassis, M. 2005, AJ, 130, 1763
Turner, J. L., & Welch, W. J. 1984, ApJ, 287, L81
van der Tak, F. F. S., van Dishoeck, E. F., & Caselli, P. 2000, A&A, 361, 327
Voronkov, M. A., Sobolev, A. M., Ellingsen, S. P., & Ostrovskii, A. B. 2005, MNRAS, 362, 995
Wilner, D. J., Wright, M. C. H., & Plambeck, R. L. 1994, ApJ, 422, 642
Wilson, T. L., Gaume, R. A., Gensheimer, P., & Johnston, K. J. 2000, ApJ, 538, 665
Wright, M. C. H., Plambeck, R. L., & Wilner, D. J. 1996, ApJ, 469, 216
Wyrowski, F., Schilke, P., Walmsley, C. M., & Menten, K. M. 1999, ApJ, 514, L43
Zapata, L. A., Rodríguez, L. F., Kurtz, S. E., & O'Dell, C. R. 2004, AJ, 127, 2252
Zapata, L. A., Ho, P. T. P., Rodríguez, L. F., Schilke, P., & Kurtz, S. 2007, A&A, 471, L59
Zapata, L. A., Schmid-Burgk, J., Ho, P. T. P., Rodríguez, L. F., & Menten, K. M. 2009, ApJ, 704, L45